Hindawi Publishing Corporation
Journal of Applied Mathematics
Volume 2013, Article ID 983051, 9 pages
http://dx.doi.org/10.1155/2013/983051

Research Article

Incomplete Phase Space Reconstruction Method Based on Subspace Adaptive Evolution Approximation

Tai-fu Li,[1] Wei Jia,[2] Wei Zhou,[1] Ji-ke Ge,[1] Yu-cheng Liu,[1] and Li-zhong Yao[1]

[1] *School of Electrical and Information Engineering, Chongqing University of Science and Technology, Chongqing 401331, China*
[2] *School of Electronic Engineering, Xi'an Shiyou University, Xi'an 710065, China*

Correspondence should be addressed to Wei Jia; jiaweifire@163.com and Wei Zhou; zhouw1985@163.com

Received 19 July 2013; Accepted 19 September 2013

Academic Editor: Baocang Ding

The chaotic time series can be expanded to the multidimensional space by phase space reconstruction, in order to reconstruct the dynamic characteristics of the original system. It is difficult to obtain complete phase space for chaotic time series, as a result of the inconsistency of phase space reconstruction. This paper presents an idea of subspace approximation. The chaotic time series prediction based on the phase space reconstruction can be considered as the subspace approximation problem in different neighborhood at different time. The common static neural network approximation is suitable for a trained neighborhood, but it cannot ensure its generalization performance in other untrained neighborhood. The subspace approximation of neural network based on the nonlinear extended Kalman filtering (EKF) is a dynamic evolution approximation from one neighborhood to another. Therefore, in view of incomplete phase space, due to the chaos phase space reconstruction, we put forward subspace adaptive evolution approximation method based on nonlinear Kalman filtering. This method is verified by multiple sets of wind speed prediction experiments in Wulong city, and the results demonstrate that it possesses higher chaotic prediction accuracy.

1. Introduction

In recent years, industrial disasters and accidents occurred frequently, the meteorological and hydrological conditions were complicated and changeable, and financial markets fluctuated drastically. These phenomena often contain chaotic characteristics [1, 2], and prediction [3] for these phenomena is imminent. For a long time, there was no scientific tool for handling this issue, because the changing mechanisms of characteristics in these phenomena were not understood very well. Hence, aiming at the chaotic characteristics, some scholars worked with structures and made a lot of new researches on the prediction of chaotic time series [4–8].

To study and deal with the measurement data of chaotic system, Kennel et al. presented the reconstruction method of phase space system. Two parameters, the embedding dimension m and delay time τ, needed to be determined before the phase space reconstruction [9, 10]. At present, time delay selection methods that are commonly used in the chaotic short-term prediction mainly include autocorrelation method [11], mutual information method [12], and singular value fraction method [13]. Calculating methods of embedding dimension mainly include saturated correlation dimension [14], false nearest neighbors method [15], and Cao's method [16]. Hu and Chen put forward the C-C method [17], which can simultaneously estimate the delay time τ and embedding dimension m with the correlation integral. Autocorrelation method extracts only linear correlation degree between time series, which is hard to be applied to high-dimensional chaos system and nonlinear dynamical system. Mutual information method, which can determine the optimal delay time by calculating the first minimal value of mutual information function, is a nonlinear analysis method, but it cannot avoid massive calculation and cannot satisfy the requirement of complicated space division. It is difficult to determine the threshold of the singular value, because the singular value fraction method is largely affected by noise. When the embedded dimension with the saturated correlation dimension is calculated, the main question is to choose the different neighborhood radius. The radius selection has certain randomness, and the result will be in large deviation with improper choice, because of the influence

of noise in the data and excessive concentration of the data. The determination of threshold has very strong subjectivity when we use false nearest neighbors method to determine the embedding dimension. There is no objective standard to determine the threshold value, especially for the experimental data, which may get a wrong result. Cao's method, an improved false nearest neighbors method, can effectively distinguish random signals and deterministic signals, and embedding dimension can be obtained through a less amount of data. C-C method is based on the statistical theory, so m cannot be precisely determined.

Researches have showed that different phase space reconstruction methods get different m and τ. Moreover, the same chaotic time series with the same kind of method in different times may get different m and τ. There is no phase space reconstruction that can obtain complete and independent phase space. After phase space reconstruction, prediction model is often established through the functional approximation method.

The prediction model based on phase space reconstruction has been used to adopt the functional approximation method based on the neural network [18–21], which has strong nonlinear fitting capability and can approximate any complex nonlinear relationships. However, since neural network is only suitable for approximation of a deterministic system, it is difficult to guarantee the time-varying system performance and ensure its generalization performance in other untrained neighborhood. Meanwhile, the prediction effect of neural network is not good, because the chaotic time series is a complex nonlinear uncertain system.

In this study, we introduce Kalman filtering to neural network model [22], inspired by Kalman iteration and Bucy and Sunahara's nonlinear extended Kalman filtering theory [23]. The subspace approximation of neural network based on the nonlinear extended Kalman filtering (EKF) has a function which is dynamic evolution approximation from one neighborhood to another. Therefore, we can constitute a phase space by choosing a kind of phase space reconstruction method, and the space may be incomplete, not separate, and can be seen as a subspace of the ideal phase space. On this basis, we put forward adaptive neural network model based on nonlinear Kalman filtering and finally realize the subspace approximation of dynamic evolution system. In addition, we simulate wind speed series in Wulong city using the proposed method. By comparing with BP neural network prediction model, the results show that our method possesses higher prediction accuracy.

The paper is organized as follows. Section 2 discusses about the subspace approximation of phase space reconstruction. In Section 3, we describe the neural network model based on nonlinear Kalman filtering. Section 4 uses practical examples and series tests to verify the proposed method, while Section 5 contains the conclusions of the present work.

2. Subspace Approximation of Phase Space Reconstruction

Reconstructing phase space by chaos theory needs to identify the chaos of time series. Single variable time series can be reconstructed into a phase space by Takens' embedding theorem in phase space reconstruction [24, 25]; that is, the original dynamical system can be restored in the sense of topological equivalence as long as the embedding dimension is sufficiently high. For the observed time series $x(1), x(2), \ldots, x(t)$, after time delay reconstruction by Takens embedding theorem, it will receive a set of space vector

$$\begin{aligned} \mathbf{X}(t) &= \{x(t), x(t+\tau), \ldots, x(t+(m-1)\tau)\}, \\ t &= 1, 2, \ldots M, \ M = N-(m-1)\tau. \end{aligned} \tag{1}$$

After phase space reconstruction, the data space is

$$\begin{bmatrix} x(1) & x(2) & \cdots & x(t) \\ x(1+\tau) & x(2+\tau) & \cdots & x(t+\tau) \\ \vdots & \vdots & \ddots & \vdots \\ x(1+(m-1)\tau) & x(2+(m-1)\tau) & \cdots & x(t+(m-1)\tau) \end{bmatrix}. \tag{2}$$

Accordingly, we acquire

$$f : \mathbf{R}^m \longrightarrow \mathbf{R}, \tag{3}$$

where f is a single-valued function. Then, we have

$$x(t+m\tau) = f(x(t), x(t+\tau), \ldots, x(t+(m-1)\tau)). \tag{4}$$

However, it cannot be really obtained as the data are often limited. Hence, $\widehat{f} : \mathbf{R}^m \rightarrow \mathbf{R}$ can only be constituted by limited measurement data, making $\widehat{f}$ sufficiently approximate to f, consequently we can get a nonlinear prediction model.

This paper employs the neural network to predict chaotic series. However, the neural network cannot readily handle the inconsistency of the phase space reconstruction because of uncertain nonlinear chaotic time series. Therefore, it is crucial to adaptively construct subspace to approximate chaotic series through the incomplete phase space. The feature of adaptive subspace approximation is that it can add new data in real time and forget old data in the process of training. Consequently, weights and thresholds of the neural network are continuously modified to realize the dynamic evolution modeling.

3. Neural Network Model Based on Nonlinear Kalman Filtering

Kalman filtering has good adaptability. It can dynamically update and forecast the system information in real time with limited data. However, it cannot be readily used for complicated nonlinear model. Meanwhile, the extended Kalman filtering (EKF) is a kind of effective method to handle nonlinear filtering.

The mathematical model of EKF is as follows:

$$\begin{aligned} \mathbf{X}_{k+1} &= f(\mathbf{X}_k, k) + \Gamma(\mathbf{X}_k, k)\mathbf{W}_k \\ \mathbf{Z}_k &= h(\mathbf{X}_k, k) + \mathbf{V}_k, \end{aligned} \tag{5}$$

where $\mathbf{W}_k$ and $\mathbf{V}_k$ are independent, zero mean, and Gaussian random processes with covariance matrices $\mathbf{Q}$ and $\mathbf{R}$, respectively. The statistical properties are as follows:

$$p(w) \sim N(0, \mathbf{Q}), \quad p(v) \sim N(0, \mathbf{R}). \tag{6}$$

EKF spreads nonlinear functions $f(\cdot)$ and $h(\cdot)$ to Taylor series around filtering value $\widehat{\mathbf{X}}_k$ and predicted value $\widehat{\mathbf{X}}_k^-$, respectively, only retaining the first-order information. Hence, the linearization model of the nonlinear system is obtained, and then we can obtain the EKF formula in nonlinear system by basic equations of Kalman filtering.

Given a forward network with N layers, the numbers of neurons in each layer are S_k ($k = 1, 2, \ldots, N$). Suppose that input layer is the first layer and output layer is the Nth layer. The weights of the kth layer neurons are W_{ij}^k ($i = 1, 2, \ldots, S_{k-1}$; $j = 1, 2, \ldots, S_k$). In order to convert the calculation of connection weights W_{ij}^k in the above problem into filter recursive estimation form, we let all of the network weights constitute the state vector

$$\mathbf{W} = \left[W_{11}^1 \cdots W_{S_1S_2}^1 W_{11}^2 \cdots W_{S_2S_3}^2 \cdots W_{11}^{N-1} W_{S_{N-1}S_N}^{N-1}\right]^T, \tag{7}$$

where state vector $\mathbf{W}$ consists of all of the weights according to the linear array, and its dimension is as follows:

$$N_W = \sum_{i=1}^{N-1} S_i S_{i+1}. \tag{8}$$

Then the state equation and measurement equation of the system can be expressed as

$$\mathbf{W}_k = \mathbf{W}_{k-1}, \tag{9}$$

$$\mathbf{Y}_{ek} = h(\mathbf{W}_k, \mathbf{X}_k) + \mathbf{V}_k = \mathbf{Y}_{rk} + \mathbf{V}_k, \tag{10}$$

where $\mathbf{Y}_{ek}$ is the expected output, $\mathbf{X}_k$ is the input vector, and $\mathbf{Y}_{rk}$ is the actual output.

The measurement noise $\mathbf{V}_k$ is assumed to be additive, white, and Gaussian, with zero mean and with covariance matrix defined by

$$E(\mathbf{V}_k) = 0, \qquad E\left(\mathbf{V}_k \mathbf{V}_k^T\right) = \mathbf{R}_k. \tag{11}$$

Suppose that the output of the jth node for the lth layer in the kth iteration is

$$O_{jk}^l = F_j^l\left(W_{jk}^l, O_k^{l-1}\right). \tag{12}$$

From (10) and (12), we have

$$\begin{aligned} \mathbf{Y}_{ek} &= h(\mathbf{W}_k, \mathbf{X}_k) + \mathbf{V}_k \\ &= F^N\left(W_k^N, F^{N-1}\left(W_k^{N-1} \cdots F^2\left(W_k^2, \mathbf{X}_k\right)\right)\right) + \mathbf{V}_k, \\ \mathbf{Y}_{ek} &= h\left(\widehat{\mathbf{W}}_k^-, \mathbf{X}_k\right) + \left.\frac{\partial h}{\partial W}\right|_{\mathbf{W}_k = \widehat{\mathbf{W}}_k^-} \left(\mathbf{W}_k - \widehat{\mathbf{W}}_k^-\right) + \mathbf{V}_k. \end{aligned} \tag{13}$$

Table 1: Extended Kalman filtering neural network algorithm.

Extended Kalman filtering neural network	
(1) Initialization	$\widehat{\boldsymbol{\theta}}_0 = E(\boldsymbol{\theta}_0) = \left[\widehat{\mathbf{W}}_0, \widehat{\mathbf{b}}_0\right]^T$ $\mathbf{P}_0 = E\left[\left(\boldsymbol{\theta}_0 - \widehat{\boldsymbol{\theta}}_0\right)\left(\boldsymbol{\theta}_0 - \widehat{\boldsymbol{\theta}}_0\right)^T\right]$
(2) Time update (forecast)	$\widehat{\boldsymbol{\theta}}_k^- = \widehat{\boldsymbol{\theta}}_{k-1}$ $\mathbf{P}_k^- = \mathbf{P}_{k-1} + \mathbf{Q}_{k-1}$
(3) Measurement update (correct)	$\mathbf{K}_k = \mathbf{P}_k^- \mathbf{H}_k{}^T \left(\mathbf{H}_k \mathbf{P}_k^- \mathbf{H}_k{}^T + \mathbf{R}_k\right)^{-1}$ $\widehat{\boldsymbol{\theta}}_k = \widehat{\boldsymbol{\theta}}_k^- + \mathbf{K}_k\left[\mathbf{Y}_{ek} - h\left(\widehat{\boldsymbol{\theta}}_k^-, \mathbf{X}_k\right)\right]$ $\mathbf{P}_k = (\mathbf{I} - \mathbf{K}_k \mathbf{H}_k)\mathbf{P}_k^-$

$\mathbf{Q}_{k-1}$ and $\mathbf{R}_k$ are process noise covariance and measurement noise covariance, respectively, $\mathbf{H}_k$ is the Jacobian matrix of observable model, $\widehat{\boldsymbol{\theta}}_k^-$ is the optimal predictive value for step k according to step $k-1$, and $\widehat{\boldsymbol{\theta}}_k$ is the optimal filter estimate for step k.

Assume that

$$\left.\frac{\partial h}{\partial W}\right|_{\mathbf{W}_k = \widehat{\mathbf{W}}_k^-} = \mathbf{H}_k, \qquad h\left(\widehat{\mathbf{W}}_k^-, \mathbf{X}_k\right) - \left.\frac{\partial h}{\partial W}\right|_{\mathbf{W}_k = \widehat{\mathbf{W}}_k^-} \widehat{\mathbf{W}}_k^- = \mathbf{C}_k. \tag{14}$$

Accordingly, the measurement equation may also be expressed as

$$\mathbf{Y}_{ek} = \mathbf{H}_k \mathbf{W}_k + \mathbf{C}_k + \mathbf{V}_k. \tag{15}$$

The Jacobian matrix of the function $h(\cdot)$ is described by

$$\mathbf{H}_k = \begin{bmatrix} \dfrac{\partial h_1}{\partial w_1} & \dfrac{\partial h_1}{\partial w_2} & \cdots & \dfrac{\partial h_1}{\partial w_n} \\ \dfrac{\partial h_2}{\partial w_1} & \dfrac{\partial h_2}{\partial w_2} & \cdots & \dfrac{\partial h_2}{\partial w_n} \\ \vdots & \vdots & \ddots & \vdots \\ \dfrac{\partial h_n}{\partial w_1} & \dfrac{\partial h_n}{\partial w_2} & \cdots & \dfrac{\partial h_n}{\partial w_n} \end{bmatrix}. \tag{16}$$

Similarly, all thresholds of the network constitute the state vector

$$\mathbf{b} = \left[b_1^1 \cdots b_{S_2}^1 b_1^2 \cdots b_{S_3}^2 \cdots b_1^{N-1} \cdots b_{S_N}^{N-1}\right]^T, \tag{17}$$

where the dimension is

$$N_b = \sum_{i=1}^{N-1} S_{i+1}. \tag{18}$$

Suppose that $\mathbf{W}$ and $\mathbf{b}$ are both state variable; that is, the state vector composed of weights and thresholds is described by

$$\begin{aligned} \boldsymbol{\theta} &= [\mathbf{W}, \mathbf{b}]^T \\ &= \left[W_{11}^1 \cdots W_{S_1S_2}^1 b_1^1 \cdots b_{S_2}^1 W_{11}^2 \cdots W_{S_2S_3}^2 b_1^2\right. \\ &\quad \left. \cdots b_{S_3}^2 \cdots W_{11}^{N-1} W_{S_{N-1}S_N}^{N-1} b_1^{N-1} \cdots b_{S_N}^{N-1}\right]^T. \end{aligned} \tag{19}$$

Kalman filtering algorithm on training weights and thresholds of the neural network is as in Table 1.

Table 2: Comparison among phase space reconstruction methods.

Parameter	Method				
	Autocorrelation	Mutual information	False nearest neighbors	Cao	C-C
τ	1	12	—	—	5
m	—	—	4	3	5

"—" means nothing.

Table 3: Parameters of the same phase space reconstruction during different time periods.

Parameter	Interval				
	T_1 ($k = 1, 2, \ldots, 600$)	T_2 ($k = 601, 602, \ldots, 1200$)	T_3 ($k = 1201, \ldots, 1800$)	T_4 ($k = 1801, \ldots, 2400$)	T_5 ($k = 2401, \ldots, 3000$)
τ	5	3	4	4	5
m	5	5	4	9	10

Table 4: Comparison among phase space reconstruction methods.

Parameter	Method				
	Autocorrelation	Mutual information	False nearest neighbors	Cao	C-C
τ	1	12	—	—	3
m	—	—	3	7	4

Table 5: Various combinations on two forecasting methods.

Model	Combination	Parameter	Forecasting
a1	Autocorrelation + false nearest neighbors	$\tau = 1, m = 3$	BPNN
b1	Autocorrelation + false nearest neighbors	$\tau = 1, m = 3$	EKFNN
a2	Mutual information + false nearest neighbors	$\tau = 12, m = 3$	BPNN
b2	Mutual information + false nearest neighbors	$\tau = 12, m = 3$	EKFNN
a3	Autocorrelation + Cao	$\tau = 1, m = 7$	BPNN
b3	Autocorrelation + Cao	$\tau = 1, m = 7$	EKFNN
a4	Mutual information + Cao	$\tau = 12, m = 7$	BPNN
b4	Mutual information + Cao	$\tau = 12, m = 7$	EKFNN
a5	C-C	$\tau = 3, m = 4$	BPNN
b5	C-C	$\tau = 3, m = 4$	EKFNN

4. Simulation Examples

4.1. Determining of Embedding Dimension and Delay Time. One of the most popular chaos logistic mapper is selected as the study object. Logistic equation is

$$x_{n+1} = \alpha x_n (1 - x_n), \quad \alpha \in [0, 4]. \tag{20}$$

The related time series are produced according to (20). It is a chaotic system when $\alpha = 4$. Assume that initial value of series is 0.1, and 4000 points are calculated. The first 1000 points are eliminated as transition phenomenon, leaving the remaining 3000 points to reconstruct phase space. Before the phase space reconstruction, we determine the embedding dimension m and delay time τ. A comparison among several methods is present in Table 2.

Obviously, the optimal embedding dimension and delay time are generally different by different methods of phase space reconstruction.

In order to verify the fact that data at different time will obtain different embedding dimension m and delay time τ with the same phase space reconstruction method, we have the following experiment.

The remaining 3000 points ($k = 1, 2, \ldots, 3000$) are divided into five parts, with time intervals T_1, T_2, T_3, T_4, and T_5, respectively. Embedding dimension and delay time are present in Table 3 by C-C method.

Apparently, the data during different time periods will acquire different embedding dimension and delay time by using the same phase space reconstruction method.

4.2. Wind Speed Chaotic Series Forecasting Simulation. Analysis about the chaotic characteristics of wind speed in the process of wind power generation has been presented in a related article [26]. We record one of the wind speed data every 10 minutes, and 150 groups of wind speed data in Wulong city are used to simulate experiments in our study.

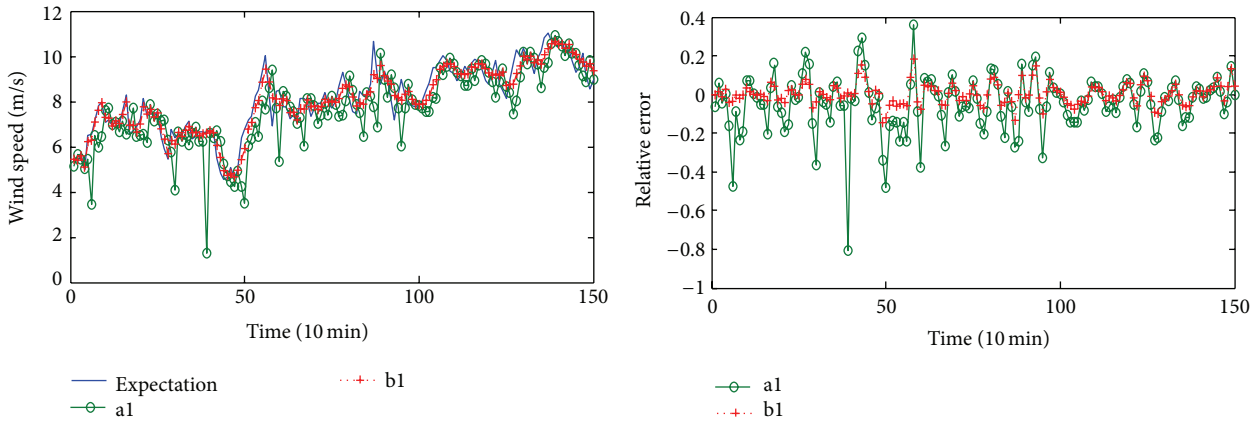

(a) The predicted wind speed data (b) Relative wind speed error

FIGURE 1: The effect comparison between a1 and b1.

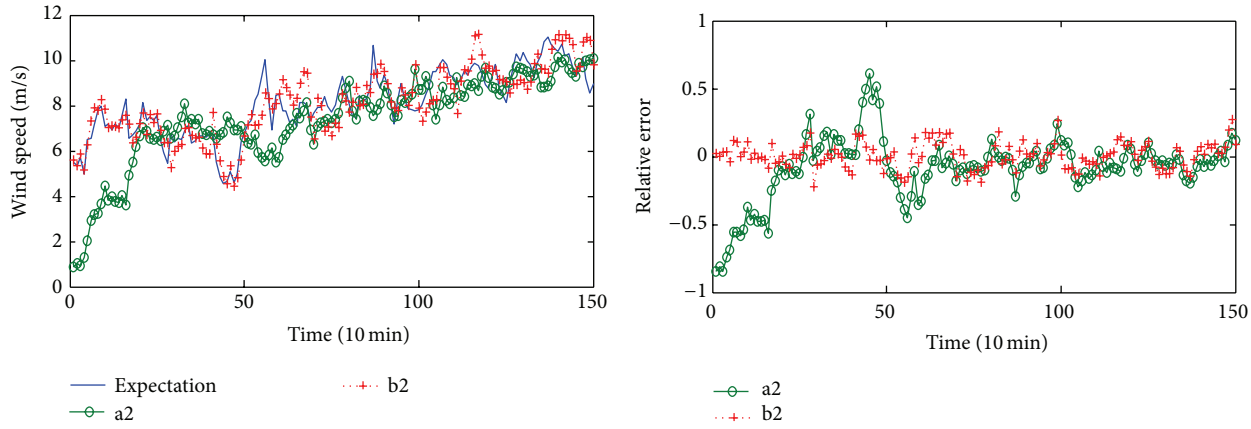

(a) The predicted wind speed data (b) Relative wind speed error

FIGURE 2: The effect comparison between a2 and b2.

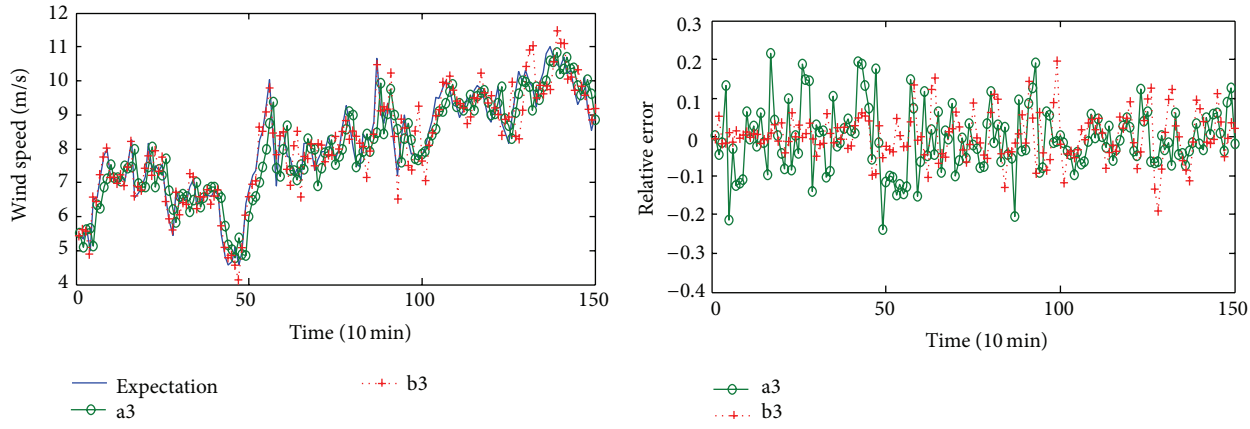

(a) The predicted wind speed data (b) Relative wind speed error

FIGURE 3: The effect comparison between a3 and b3.

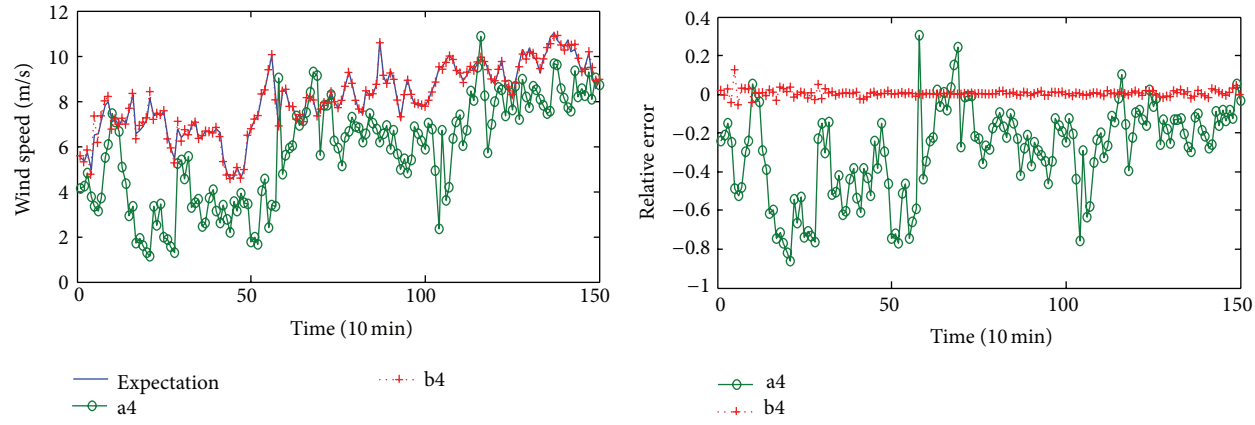

(a) The predicted wind speed data (b) Relative wind speed error

FIGURE 4: The effect comparison between a4 and b4.

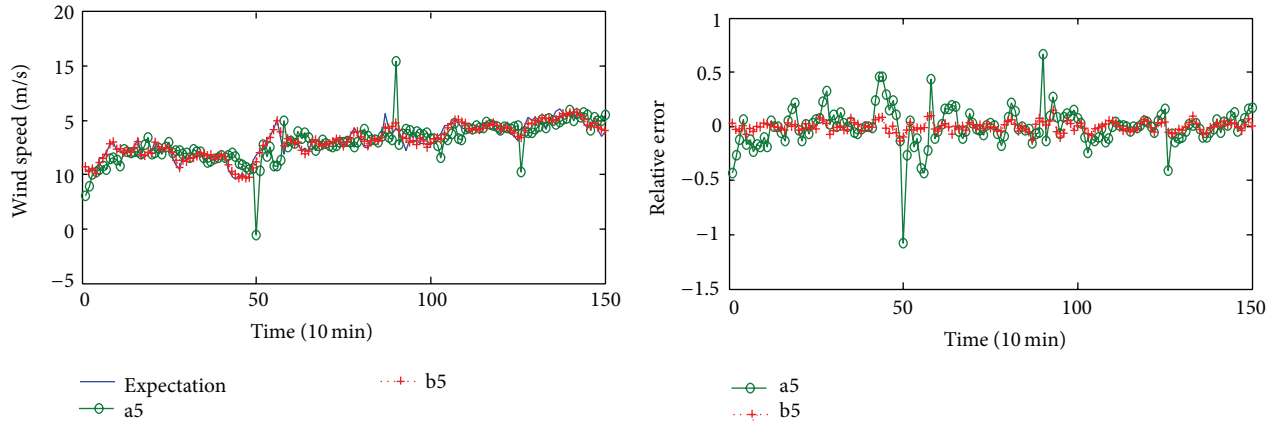

(a) The predicted wind speed data (b) Relative wind speed error

FIGURE 5: The effect comparison between a5 and b5.

We obtain the corresponding m and τ by different phase space reconstruction methods, as shown in Table 4.

Various combinations are present in Table 5.

Wind speed prediction [27, 28] of chaotic time series about neural network model usually extracts phase space reference points as the BP neural network training samples on the basis of phase space reconstruction. We establish the neural network model based on nonlinear Kalman filtering, including two parts: predict wind speed and constantly modify weights and thresholds of the neural network by Kalman recursion. In this paper, BPNN model in the same structure is employed to forecast wind speed time series, in order to illustrate the validity of EKFNN on predicting the chaotic time series. The same 150 groups of wind speed data are used to simulate experiments. The predicted curves and error curves are shown in Figures 1, 2, 3, 4, and 5.

Comparisons among several models in four indices are present in Table 6.

We list 12 groups, a total of 2 hours of wind speed forecasting results in two methods, under the same phase space reconstruction. Compare the prediction performance in the next 10 min, 20 min, 30 min, and up to, 120 min.

TABLE 6: Different wind speed model index.

Model	Error			
	MAE	MRE	MSE	SSE
a1	0.8482	0.1076	1.3786	206.7967
b1	0.3365	0.0416	0.1919	28.7834
a2	1.2279	0.1674	2.9614	444.2152
b2	0.6190	0.0759	0.6209	93.1357
a3	0.5106	0.0656	0.4089	61.3361
b3	0.3783	0.0458	0.2654	39.8130
a4	2.4005	0.3079	8.4766	$1.2715e+003$
b4	0.0852	0.0110	0.0177	2.6584
a5	0.8952	0.1173	1.7970	269.5495
b5	0.2867	0.0357	0.1359	20.3850

MAE, MRE, MSE, and SSE are Mean Absolute Error, Mean Relative Error, Mean Square Error, and Sum of Squared Error, respectively.

Table 7: Observed wind speed data and predicted data.

Time (min)	Observed value (m/s)	Predicted value (m/s)	Relative error (%)	Predicted value (m/s)	Relative error (%)
		a1		b1	
10	10.4900	10.0801	3.9561	10.5101	0.1823
20	10.3700	9.9783	3.7762	10.4011	0.2630
30	10.6900	10.1024	5.4902	10.4621	2.1476
40	10.2100	10.8802	6.5374	10.6202	4.0235
50	10.3000	9.1424	11.2402	10.1531	1.4947
60	9.8000	10.3508	5.6401	10.2210	4.2446
70	9.3000	8.6881	6.5810	9.6032	3.2585
80	9.4900	8.1883	13.7201	9.3163	1.8295
90	10.1100	9.6013	5.0321	9.7631	3.4282
100	9.2100	10.4726	13.7200	10.0300	8.9132
110	8.5500	7.2082	15.6903	8.8621	3.6533
120	9.0000	7.0824	21.3101	8.5470	5.0347
		a2		b2	
10	10.4900	9.6930	7.5977	10.4785	0.1095
20	10.3700	10.4006	0.2955	10.4249	0.5292
30	10.6900	10.0489	5.9968	10.4992	1.7845
40	10.2100	10.5699	3.5250	10.3357	1.2311
50	10.3000	10.2559	0.4285	10.2518	0.4675
60	9.8000	10.1445	3.5151	10.1132	3.1960
70	9.3000	9.2583	0.4488	10.0703	8.2826
80	9.4900	9.8944	4.2609	9.9547	4.8963
90	10.1100	10.6937	5.7739	9.7503	3.5580
100	9.2100	11.4420	24.2351	9.5212	3.3787
110	8.5500	11.8315	38.3804	9.1823	7.3954
120	9.0000	11.2543	25.0475	9.3012	3.3463
		a3		b3	
10	10.4900	10.9775	4.6468	10.7194	2.1870
20	10.3700	10.4931	1.1872	10.4277	0.5567
30	10.6900	10.3878	2.8269	10.4168	2.5559
40	10.2100	13.7393	34.5672	10.1893	0.2032
50	10.3000	9.8085	4.7716	10.2918	0.0793
60	9.8000	12.1826	24.3126	10.0993	3.0540
70	9.3000	9.7924	5.2943	9.8370	5.7739
80	9.4900	9.3521	1.4529	9.6689	1.8855
90	10.1100	14.5803	44.2168	9.7772	3.2920
100	9.2100	14.6095	58.6264	9.5805	4.0233
110	8.5500	8.6425	0.0821	9.3442	9.2884
120	9.0000	9.7379	8.1988	9.3314	3.6817
		a4		b4	
10	10.4900	8.9295	14.8759	10.1137	3.5868
20	10.3700	9.2037	11.2466	9.7344	6.1296
30	10.6900	8.6494	19.0887	10.3308	3.3597
40	10.2100	8.5516	16.2426	9.9803	2.2501
50	10.3000	9.3038	9.6717	10.5685	2.6064
60	9.8000	8.7467	10.7479	10.1183	3.2477
70	9.3000	8.7126	6.3161	9.7779	5.1391

Table 7: Continued.

Time (min)	Observed value (m/s)	Predicted value (m/s)	Relative error (%)	Predicted value (m/s)	Relative error (%)
80	9.4900	8.6188	9.1802	9.8413	3.7021
90	10.1100	9.4713	6.3176	10.9886	8.6901
100	9.2100	9.3204	1.1992	8.8816	3.5657
110	8.5500	9.5029	11.1452	8.2497	3.5118
120	9.0000	9.6909	7.6768	8.8558	1.6017
		a5		b5	
10	10.4900	10.1227	3.5017	10.4227	0.6412
20	10.3700	10.5150	1.3985	10.4890	1.1473
30	10.6900	10.3714	2.9805	10.6268	0.5909
40	10.2100	10.1625	0.4652	10.5638	3.4649
50	10.3000	10.5236	2.1705	10.4778	1.7260
60	9.8000	10.5366	7.5159	10.1741	3.8174
70	9.3000	9.8748	6.1807	9.8224	5.6174
80	9.4900	9.4500	0.4217	9.6744	1.9432
90	10.1100	9.7279	3.7794	9.8950	2.1267
100	9.2100	8.9728	2.5755	9.6195	4.4458
110	8.5500	9.3838	9.7519	9.2464	8.1455
120	9.0000	9.3328	3.6973	9.0710	0.7889

Comparisons among several prediction results in two methods are present in Table 7.

Figures 1–5 show that relative error of wind speed prediction by EKF neural network is much smaller than that by BP neural network, through observing the future wind speed prediction of 150 groups. As can be seen in Table 6, the prediction effects are largely different by different kinds of phase space reconstruction methods. Four performance indices, which are Mean Absolute Error (MAE), Mean Relative Error (MRE), Mean Square Error (MSE), and Sum of Squared Error (SSE), of EKF neural network, are also far less than those of corresponding general neural network.

Apparently, EKF neural network can solve the inconsistency problem of phase space reconstruction and approximate chaotic time series well through subspace. The neural network model based on EKF has outstanding adaptability, so it can predict the wind speed chaotic time series with higher precision, compared with BP neural network.

Furthermore, we can conclude that in Table 7, prediction accuracy of EKF neural network is higher than that of BP neural network, by comparing the prediction performance of wind speed in the next 10 min, 20 min, 30 min, and up to, 120 min. It demonstrates that EKF neural network model, which has better dynamic adaptability, can better the prediction of wind speed time series with nonlinear chaotic characteristics. Therefore, the proposed phase space reconstruction method of the adaptive evolution approximation in this paper is an effective approach.

5. Conclusion and Further Work

The phase space reconstruction cannot meet characteristics of the completeness and independence, and the results with different reconstruction methods are obviously inconsistent. The reconstructed phase space is a subspace of the ideal space. If a subspace approximation can make the real-time dynamic evolution, then the initial constructed phase space, for which the evolution is adaptive subspace approximation, can finally approximate to the ideal phase space much better.

In this paper, neural network model based on nonlinear Kalman filter is established, by dynamic adaptivity of nonlinear Kalman filter. The model will add new samples in real time and gradually eliminate previous data, as a moving samples window, and the evolution of the training sample continually updates weights and thresholds of the neural network. As a result, adaptive subspace approximation is implemented by reconstructed incomplete phase space.

The optimized plan, which combines the nonlinear Kalman filter with neural network, sufficiently utilizes the nonlinear approximation capability of neural network and dynamic adaptive ability of real-time update correction of nonlinear Kalman filter. Consequently, it can realize subspace adaptive evolution approximation and solve the inconsistency problem of phase space reconstruction. Therefore, it is a nice direction in research into chaotic prediction. Future research can be performed in a number of areas. It provides a good technical support in studying problems of meteorology, hydrology, and finance fields.

Acknowledgments

This work was supported by the National Science Foundation of China (no. 51075418), the National Science Foundation of China (no. 61174015), Chongqing CMEC Foundations of China (no. CSTC 2013jjB40007), and Chongqing Scientific Personnel Training Plan of China (no. CSTC 2013kjrc-qnrc40008).

References

[1] G. Kaddoum, F. Gagnon, P. Chargé, and D. Roviras, "A generalized BER prediction method for differential chaos shift keying system through different communication channels," *Wireless Personal Communications*, vol. 64, no. 2, pp. 425–437, 2012.

[2] B. Sivakumar, "Chaos theory in geophysics: past, present and future," *Chaos, Solitons & Fractals*, vol. 19, no. 2, pp. 441–462, 2004.

[3] P. A. Mastorocostas, J. B. Theocharis, and A. G. Bakirtzis, "Fuzzy modeling for short term load forecasting using the orthogonal least squares method," *IEEE Transactions on Power Systems*, vol. 14, no. 1, pp. 29–36, 1999.

[4] H. Y. Yang, H. Ye, G. Wang, J. Khan, and T. Hu, "Fuzzy neural very-short-term load forecasting based on chaotic dynamics reconstruction," *Chaos, Solitons & Fractals*, vol. 29, no. 2, pp. 462–469, 2006.

[5] B. Sivakumar, "A phase-space reconstruction approach to prediction of suspended sediment concentration in rivers," *Journal of Hydrology*, vol. 258, no. 1–4, pp. 149–162, 2002.

[6] A. Porporato and L. Ridolfi, "Nonlinear analysis of river flow time sequences," *Water Resources Research*, vol. 33, no. 6, pp. 1353–1367, 1997.

[7] P. Zhao, L. Xing, and J. Yu, "Chaotic time series prediction: from one to another," *Physics Letters A*, vol. 373, no. 25, pp. 2174–2177, 2009.

[8] H. D. I. Abarbanel, *Analysis of Observed Chaotic Data*, Springer, New York, NY, USA, 1996.

[9] M. B. Kennel, R. Brown, and H. D. I. Abarbanel, "Determining embedding dimension for phase-space reconstruction using a geometrical construction," *Physical Review A*, vol. 45, no. 6, pp. 3403–3411, 1992.

[10] H. Ma and C. Han, "Selection of embedding dimension and delay time in phase space reconstruction," *Frontiers of Electrical and Electronic Engineering in China*, vol. 1, no. 1, pp. 111–114, 2006.

[11] B. Chen, G. Liu, J. Tang et al., "Research on chaotic sequence autocorrelation by phase space method," *Journal of the University of Electronic Science and Technology of China*, vol. 39, no. 6, pp. 859–863, 2010.

[12] A. Jiang, X. Huang, Z. Zhang, J. Li, Z.-Y. Zhang, and H.-X. Hua, "Mutual information algorithms," *Mechanical Systems and Signal Processing*, vol. 24, no. 8, pp. 2947–2960, 2010.

[13] N. Abu-Shikhah and F. Elkarmi, "Medium-term electric load forecasting using singular value decomposition," *Energy*, vol. 36, no. 7, pp. 4259–4271, 2011.

[14] C. Gao and X. Liu, "Chaotic identification of BF ironmaking process I: the calculation of saturated correlative dimension," *Acta Metallurgica Sinica*, vol. 40, no. 4, pp. 347–350, 2004.

[15] I. M. Carrión and E. A. Antúnez, "Thread-based implementations of the false nearest neighbors method," *Parallel Computing*, vol. 35, no. 10-11, pp. 523–534, 2009.

[16] J. Hite Jr., *Learning in Chaos*, Gulf Professional Publishing, Amsterdam, The Netherlands, 1999.

[17] Y. Hu and T. Chen, "Phase-space reconstruction technology of chaotic attractor based on C-C method," *Journal of Electronic Measurement and Instrument*, vol. 35, no. 10-11, pp. 425–430, 2012.

[18] D. A. Fadare, "The application of artificial neural networks to mapping of wind speed profile for energy application in Nigeria," *Applied Energy*, vol. 87, no. 3, pp. 934–942, 2010.

[19] S. Salcedo-Sanz, A. M. Ángel M. Pérez-Bellido, E. G. Ortiz-García, A. Portilla-Figueras, L. Prieto, and D. Paredes, "Hybridizing the fifth generation mesoscale model with artificial neural networks for short-term wind speed prediction," *Renewable Energy*, vol. 34, no. 6, pp. 1451–1457, 2009.

[20] D. C. Dracopoulos, *Evolutionary Learning Algorithms for Neural Adaptative Control*, Springer, London, UK, 1997.

[21] J. Xue and Z. Shi, "Short-time traffic flow prediction based on chaos time series theory," *Journal of Transportation Systems Engineering and Information Technology*, vol. 8, no. 5, pp. 68–72, 2008.

[22] H. Yang, J. Li, and F. Ding, "A neural network learning algorithm of chemical process modeling based on the extended Kalman filter," *Neurocomputing*, vol. 70, no. 4–6, pp. 625–632, 2007.

[23] R. S. Bucy and K. D. Senne, "Digital synthesis of non-linear filters," *Automatica*, vol. 7, no. 3, pp. 287–298, 1971.

[24] J. Wang and Y. Xie, "Solar radiation prediction based on phase space reconstruction of wavelet neural network," *Procedia Engineering*, vol. 15, no. 1, pp. 4603–4607, 2011.

[25] H. Kantz and T. Schreiber, *Nonlinear Time Series Analysis*, Cambridge University Press, Cambridge, UK, 1997.

[26] T. E. Karakasidis and A. Charakopoulos, "Detection of low-dimensional chaos in wind time series," *Chaos, Solitons & Fractals*, vol. 41, no. 4, pp. 1723–1732, 2009.

[27] P. Louka, G. Galanis, N. Siebert et al., "Improvements in wind speed forecasts for wind power prediction purposes using Kalman filtering," *Journal of Wind Engineering and Industrial Aerodynamics*, vol. 96, no. 12, pp. 2348–2362, 2008.

[28] M. Poncela, P. Poncela, and J. R. Perán, "Automatic tuning of Kalman filters by maximum likelihood methods for wind energy forecasting," *Applied Energy*, vol. 108, no. 12, pp. 349–362, 2013.